PRAMANA
—journal of
physics

Vol. 50, No. 6,
June 1998
pp. 607–615

Photoionization of some closed shell atoms and ions

H S CHAKRABORTY, P C DESHMUKH, S T MANSON* and D W LINDLE†
Department of Physics, Indian Institute of Technology, Chennai 600 036, India
*Department of Physics and Astronomy, Georgia State University, GA 30303, USA
†Department of Chemistry, University of Nevada, Las Vegus, NV 89154-4003, USA

Abstract. Dipole-allowed single photoionization of some closed shell atoms and ions has been investigated in the relativistic random-phase approximation (RRPA). Application of relativistic-multichannel quantum defect theory (RMQDT) is made together with RRPA to analyse autoionizing resonances. Analysis points to the importance of interchannel coupling in high energy photoionization and reveals various degeneracies in relativistic atomic spectra to influence the low energy dynamics. Interesting threshold behavior in photoelectron spin polarization has been seen. Prospective future studies have been indicated.

Keywords. Atomic physics; photoabsorption.

PACS No. 32.80

1. Introduction

Photoionization is considered to be a useful method to carry out spectroscopical and dynamical investigations on atomic systems, as the information thus obtained is of relatively pure form. This is simply because the photon field couples very weakly with the system to induce minimal perturbation. Moreover, since the final channel comprises of only the photoelectron, the incoming photon being absorbed by the target, the analysis becomes rather simple.

Over the last several decades there have been many experimental studies [1] on atomic photoionization to understand the dynamics of the process. In recent times, owing to the advent of experimental technology, a renewed interest is seen in high precision measurements. For a long time, the main obstacle to extensive experimental research at energies as low as x-ray range has been the limitation of discrete characteristic lines from x-ray tubes. Currently available x-ray synchrotron radiation facilities remove this obstacle and provide the experimentalists with an intense, tunable, and highly polarized x-ray beam. Laboratory research thus receives a major boost from such developments toward high resolution photoionization measurements [2, 3]. Measurements of photoionization angular distribution, that require an angle-resolved spectroscopy, have revealed interesting new information. We illustrate in the following two most recent works on non-resonant photoionization. Importance of effects beyond conventional dipole effects for inner-shell at relatively low energy photoemission has been realised [4, 5]. For argon 1s, krypton 2s, and krypton 2p photoemission, pronounced non-dipole asymmetries with respect to the direction of photon propagation have been seen [4]. With the increase of photon-energy

this asymmetry is found to be enhanced with the emission pattern being progressively forward skewed. Further, most recent experiments [5] have shown multipole influence in angular distribution for valence photoionization at energies significantly lower than what was considered earlier. These findings, therefore, set a trend of deviating from the conventional approach in interpreting angle-resolved photoemission data. There have also been some recent studies on autoionization resonances by high resolution photoelectron spectroscopy using synchrotron photon sources [6]. Experimental studies on $2s \rightarrow np$ resonances in $2p$ photoionization of neutral neon and some ions isoelectronic to it are also in progress [7].

In the theoretical realm also, interest in these investigations can clearly be noticed. Motivation comes, on one hand, from the need to support and complement new experimental knowledge, and on the other hand, from the necessity to investigate in detail the role of many-body effects to influence photoionization dynamics. Availability of powerful computers has invigorated such activities by enabling extensive application of *ab initio* methodologies that incorporate all important correlations. The significance of relativistic effects, that often appears rather strikingly in precision measurements, underlines the need of a relativistic formulation to address the problem. Among the simplest and most widely applied of various many-body techniques is the relativistic random-phase approximation (RRPA) [8, 9]. By treating certain types of correlations to all orders, the analysis of photoexcitation or photoionization can be reduced to the solution of a set of integro-differential RRPA equations [8]. RRPA has been widely used in the atomic photoionization at low energies [8, 9], and in the intermediate energies both over the non-resonant and autoionizing resonance region [10].

Using the RRPA methodology, we have recently completed a number of investigations on single-ionization from several closed shell neutral atoms and from some ions isoelectronic to them. Section 2 briefly describes the working formulas of all dipole allowed photoionization parameters in a convenient interaction geometry. In § 3, we discuss the results. We conclude the article in § 4 by briefly indicating future programs that spawn out of the current activities.

2. Photoionization dynamical parameters

We consider the incident photon to be in its most general polarization state. It is also assumed that the target system is unpolarized and that the polarization of the residual ion is not observed. This can be ensured by averaging over the polarization of the target and summing up the polarization of the residual core. The polarization of photon radiation can now be defined with respect to a target-fixed coordinate frame XYZ such that the Z axis is in the direction of the photon flux. Conventionally, the X axis is chosen to coincide with the linear polarization vector or with one of the principal axes of elliptically polarized photons. On the other hand, the photoelectron polarization is defined with respect to another coordinate frame xyz that is obtained by affecting a rotational transformation on the fixed frame XYZ with the Euler angles $(\phi, \theta, 0)$ such that the z axis is in the direction of photoelectron momentum and the y axis is perpendicular to both Z and z axes. The angular distribution and spin polarization of the photoelectrons ejected from $n\kappa$ subshell [n is the principal quantum number and the quantum number $\kappa = \mp(j + 1/2)$

for $j = (l \pm 1/2)$, j and l being the one-electron total and orbital angular momentum quantum numbers] can thus be given, in the framework of the dipole approximation, by the following set of equations [11]:

$$\frac{d\sigma}{d\Omega}(\theta, \phi) = \frac{\sigma}{4\pi} F(\theta, \phi), \tag{1}$$

$$P_x(\theta, \phi) = [\xi p \sin(2\alpha) + \eta p \cos(2\alpha) \sin(2\bar{\phi})] \sin\theta / F(\theta, \phi), \tag{2}$$

$$P_y(\theta, \phi) = \eta[1 + p \cos(2\alpha) \cos(2\bar{\phi})] \sin\theta \cos\theta / F(\theta, \phi), \tag{3}$$

$$P_z(\theta, \phi) = \zeta p \sin(2\alpha) \cos\theta / F(\theta, \phi), \tag{4}$$

where

$$F(\theta, \phi) = 1 - \tfrac{1}{2}\beta[P_2(\cos\theta) - \tfrac{3}{2} p \cos(2\alpha) \cos(2\bar{\phi}) \sin^2\theta] \tag{5}$$

in which $P_2(\cos\theta)$ is the well-known Legendre polynomial of second order. In eqs (1–5), p specifies the degree of polarization [i.e. $p = 1$ for pure polarized, $0 < p < 1$ for mixed polarized and $p = 0$ for unpolarized photon], the angle α $(-\pi/2 < \alpha < \pi/2)$ determines the type of polarization [12] and $\bar{\phi} = \phi - \gamma$, the azimuthal angle of the photoelectron direction with respect to the linear polarization vector, or with respect to the principal axis ($k \cos\alpha$) of elliptically polarized photon, wherein γ $(0 \leq \gamma < \pi)$ is the azimuthal orientation of the polarization [12]. Thus, the dipole photoionization can be completely described, in general, by a set of five dynamical parameters σ, β, ξ, η and ζ, in which σ is the partial cross section, β is the angular distribution asymmetry parameter and the remainders are the photoelectron spin polarization parameters. It is now possible to express these dynamical parameters in terms of certain reduced dipole matrix elements [8] in RRPA.

3. Results and discussion

In this section we classify our results to be presented in two groups as follows:

3.1 *Interchannel coupling effects*

Dramatic effects of interchannel coupling are illustrated below from a recent study of photoionization of atomic neon [13, 14]. The cross section and angular distribution asymmetry parameter of neon $2p$ photoionization were calculated at four levels of interchannel coupling approximations: (i) coupling of all the relativistic dipole-allowed excitation/ionization channels arising from $2p$, $2s$, and $1s$; (ii) from $2p$ and $2s$ only; (iii) from $2p$ and $1s$ only; and (iv) from $2p$ alone. Such implementation of the coupling scheme in the truncated RRPA gives a handle on selective determination of the effect of couplings between different channels. The results for the angular distribution asymmetry parameter β are shown in figure 1 [14]. All four levels of calculations are in reasonable accord with each other at the lowest energies considered, understandably due to the dominance of $2p$ ionization matrix element over that of the $2s$ resulting in an inappreciable interchannel coupling contribution. With increasing photon energy, however, the $2p$ matrix elements fall off more rapidly than the $2s$. This translates into two groups of

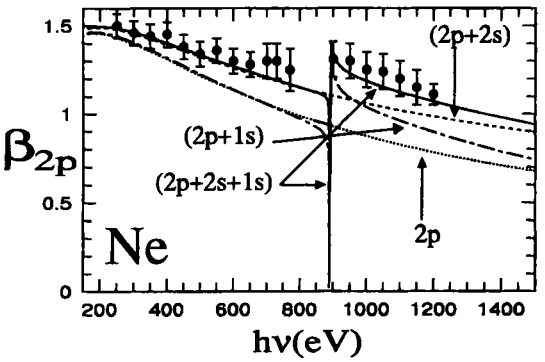

Figure 1. Photoelectron angular distribution asymmetry parameter β for Ne $2p$ calculated using RRPA formalism with the single excitation channels arising from $2p$, $2s$, and $1s$ coupled (solid line): $2p$ and $2s$ (dashed line); $2p$ and $1s$ (dash-dotted line); and $2p$ alone (dotted line). The experimental points are from ref. [5].

results around 500 eV range. The two calculations with $2p$ and $2s$ coupled agree with each other, and the residual two agree with each other but disagree with the former group. This clearly points at the $2p$ and $2s$ interchannel coupling being responsible for the difference. While the trend is interrupted at about 870 eV where $1s$ photoionization channels open, at higher energies, however, it resumes. Recent measurements [5] of β show excellent agreement with results that include $2s$ channels. Our single-particle calculation of β (not shown) at high energies is virtually indistinguishable from the $2p$ calculation alone, because of negligible contribution from intrachannel coupling. At highest energy considered we see, however, about a 30% shift of β from the single-particle predictions indicating, contrary to the conventional understanding, inadequacy of single-particle model and importance of coupling with energetically neighboring channels at high enough energies.

Similar calculations on $3p$ photoionization of argon [15] further confirm our finding. Cross section and angular distribution for valence $3p$ photoelectrons of argon have been calculated in five levels of interchannel coupling scheme: all single ionization dipole channels arising from (i) $3p$, $3s$, $2p$, $2s$ and $1s$ (full RRPA), (ii) $3p$ and $3s$, (iii) $3p$ and $2p$, (iv) $3p$ and $2s$ and (v) only $3p$. The scheme (v), as in the case of neon only-$2p$ calculations, yields virtually similar results to independent particle method at *high enough* energy. Except at $2p$ (binding energy $\sim$ 260 eV) and $2s$ (binding energy $\sim$338 eV) resonance regions, the results fall in two distinct classes: (a) one in which coupling with channels from $3s$ subshell is included and (b) in which it is not. For photoelectron angular distribution asymmetry parameter β_{3p} (figure 2), the difference between these two classes of result is about 10% at the highest energies considered. Corresponding cross section results, as presented in figures 3a, b, also exhibit similar qualitative behavior as β. The local 'minimum' near 50 eV seen in figure 3a is the well-known 'Cooper minimum' whereas the 'spikes' seen in figures 2 and 3a near $\sim$ 230 eV and $\sim$ 338 eV are respectively due to $2p \rightarrow ns, nd$ and $2s \rightarrow np$ excitations. The high energy dynamics seen in figures 2 and 3 emphasize the importance of coupling of photoionization channels under consideration with channels from energetically neighboring thresholds to accurately describe high energy nl $(l > 0)$ photoionization of atoms.

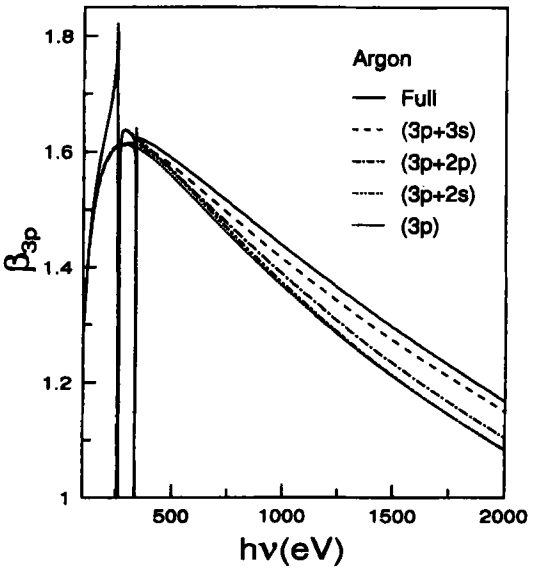

Figure 2. Angular distribution asymmetry parameter β for Ar $3p$ photoionization calculated via RRPA by coupling between channels arising from (i) $3p$, $3s$, $2p$, $2s$ and $1s$ (solid line), (ii) $3p$ and $3s$ (dashed line), (iii) $3p$ and $2p$ (dash-dotted line), (iv) $3p$ and $2s$ (dash-double-dotted line) and (v) only $3p$ (dotted line).

3.2 *Autoionizing resonances, threshold photoionization and photoelectron spin polarization*

Autoionizing resonances occur in photoionization dynamical parameters due to the interference of the continuum and discrete channels. At energy where an innershell excitation occurs the phase of photoelectron outgoing wave exhibits rapid spectral variation to induce such a resonance.

Detail study on the autoionizing resonances for various closed shell systems and their isoelectronic sequences has recently been carried out by us. RRPA has been used to determine *ab initio* a set of energy insensitive photoabsorption parameters, called the quantum defect parameters. These are then employed in the relativistic-multichannel quantum defect theory (RMQDT), as described in ref. [16], to make an analysis of the autoionizing resonances. The calculated quantum defect parameters are the eigenamplitudes (D_α), the eigenquantum defects (μ_α), and the expansions of the eigenvectors in the jj basis, the $[U_{jj,\alpha}]$-matrix. These quantum defect parameters have subsequently been utilized to calculate all physical parameters of ionization. Elegant techniques have been developed to understand the real characteristic of the angular momentum coupling of the excited electron with the residual core.

A study on autoionizing resonances resulting from $1s \rightarrow np$ excitation and appearing in $2s$ photoionization of atomic beryllium has lately been completed [17]. Similar studies [13, 18] for valence photoionization on the neon, magnesium and xenon isoelectronic sequence and xenon isonuclear sequence will be published shortly.

Preliminary calculations were carried out recently [13] for many members of the neon isoelectronic sequence. The photoionization cross section, photoelectron angular

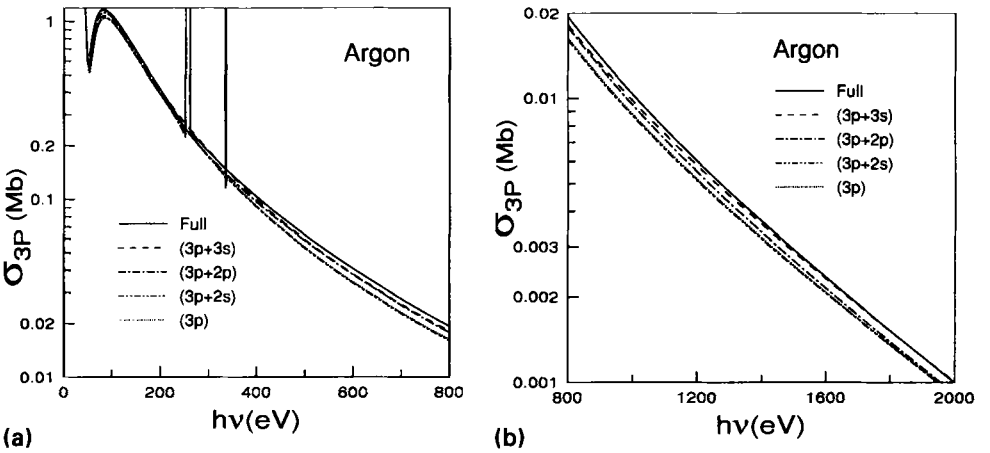

Figure 3. Cross section for Ar $3p$ photoionization calculated using the RRPA by coupling between channels arising from (i) $3p$, $3s$, $2p$, $2s$ and $1s$ (solid line), (ii) $3p$ and $3s$ (dashed line), (iii) $3p$ and $2p$ (dash-dotted line), (iv) $3p$ and $2s$ (dash-double-dotted line) and (v) only $3p$ (dotted line); (**a**) for energy range from $3p$ threshold through 800 eV, and (**b**) for the range 800 eV through 2 KeV.

distribution asymmetry parameter, and the photoelectron spin polarization parameters for background photoionization of low energy $2p_{\frac{3}{2}}$ and $2p_{\frac{1}{2}}$ electrons were computed. Two-shell correlations between valence $2p$ shell and neighboring $2s$ shell were included. These preliminary studies showed that the low-energy threshold behavior of photoionization cross-section of the $2p$ shell is influenced by the centrifugal barrier to the final state continuum-d states in the case of Ne for which a 'shape resonance' is seen in the threshold area. This was seen to become weaker across the next few members of the isoelectronic sequence. For a group of ions, for example Si^{4+}, the results just above their respective $2p_{\frac{1}{2}}$ thresholds were seen to be unusual in that the cross-section was seen to rise sharply above the ionization threshold and then fall when interchannel coupling with photoexcitation channels from the $2s$ shell was included, while this feature was lost when intershell $(2s, 2p)$ correlations were excluded whence the photoionization cross-section was seen to fall monotonically above the threshold.

We have carried out a very detailed RRPA + RMQDT analysis of the photoabsorption process in the threshold region of several members of the neon isoelectronic sequence. For each ion of the isoelectronic sequence, the threshold feature essentially originates from a 'perturbation' caused by an excited state corresponding to a $2s \rightarrow np$ transition which although occurs in the discrete spectrum of $2p_{\frac{1}{2}} \rightarrow ns, nd$ channels lies close enough to the $2p_{\frac{1}{2}}$ ionization threshold as to influence the continuum. It turns out that for Si^{4+} (see figure 4) the $2s \rightarrow 3p$ excited state resides very near the $2p_{\frac{1}{2}}$ threshold thus causing maximum interference. As seen in figure 4, the threshold profile is very rich in $2s \rightarrow np$ autoionization resonances and on-going experiments [7] show very encouraging agreement with our results.

The four spin polarization parameters ζ, η, ξ and δ, described in equations (2)–(5), were calculated using RRPA for valence $3p$ and inner $2p$ photoionization of atomic argon over the non-resonant region; results are presented in figures 5a, b respectively. $3p$ photoelec-

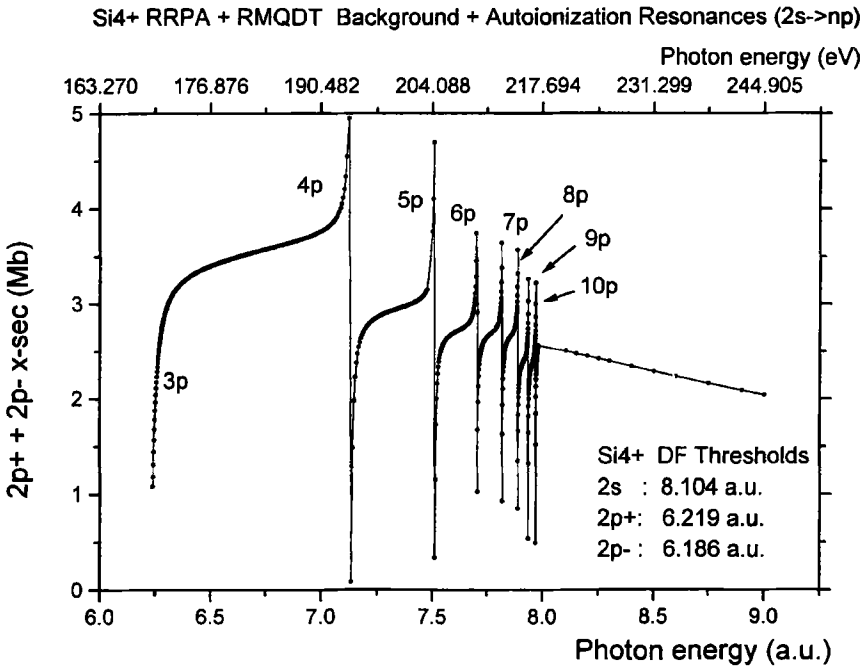

Figure 4. Photoionization cross section for Si^{4+} $2p$ plotted above the $2p_{\frac{1}{2}}$ threshold which shows $2p \rightarrow ns$ autoionizing resonances.

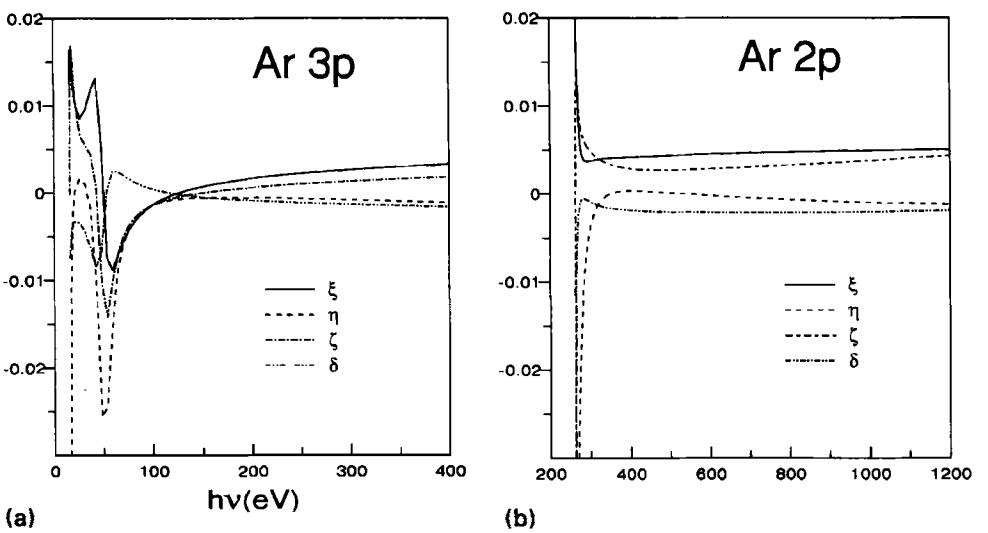

Figure 5. Non-resonant spin polarization parameters ξ (solid curve), η (dashed curve), ζ (dash-dotted curve), and δ (dash-dot-dotted curve) are drawn as a function of photon energy for Ar; (**a**) for valence $3p$ photoionization and (**b**) for $2p$ photoionization.

tron spin polarization of argon (figure 5a) shows interesting threshold features in the region of the "Cooper minimum" seen in figure 3a. Argon $2p$ photoelectron spin polarization parameters also shows (figure 5b) some interesting threshold structure. A more detailed study of photoelectron spin polarization which will provide deeper knowledge about the role of correlation dynamics is under way.

4. Conclusions

Our recent photoionization studies yield some new and interesting insights about atomic photoprocesses. Importance of interchannel coupling stresses the inadequacy of the single-particle models at even photon energies well above the threshold, and interestingly, this feature becomes more pronounced as one goes higher still above the threshold. The present analysis of atomic photoionization is prototype of similar processes occurring in molecules and for condensed matter targets. Studies of autoionizing resonances and the quantitative knowledge of the coupling character of the corresponding photoexcited electron with residual core over an isoelectronic sequence provides knowledge on the single-electron bound state spectrum and its evolution as a function of Z. Influence of resonances on threshold photoionization is also a very important finding of the present work as is seen, for instance, in the case of Si^{4+} valence photoemission. Study of photoelectron spin polarization also finds substantial importance in understanding correlation dynamics in target atomic systems.

These results along with recent measurements are encouraging for future research programs. Excellent agreement of RRPA calculations with measurements in dipole frame [5,14] indicates the strength of the methodology. Growing experimental consensus on the significance of non-dipole contribution also at relatively low energies [4, 5] is a major impetus for further theoretical investigations. Theoretical studies of non-dipole photoionization along with the inclusion of core relaxation effects will constitute a major part of future endeavors.

Acknowledgement

The authors are grateful to Professor W R Johnson for providing them the RRPA and RMQDT codes. The present work was partially supported by a National Science Foundation (USA) grant at IIT, Chennai. They also acknowledge the facilities provided by IIT, Chennai.

References

[1] V Schmidt, *Rep. Prog. Phys.* **55**, 1483 (1992)
[2] N Berrah, B Langer and A Farhat, *Indian J. Phys.* **B71**, 223 (1997)
[3] D W Lindle, O Hemmers, P Glans, D L Hansen, H Wang, S B Whitfield, R Wehlitz, J C Levin, I A Sellin and R C C Perera, *Indian J. Phys.* **B71**, 325 (1997)
[4] M Jung, B Krässig, D S Gemmell, E P Kanter, T LeBrun, S H Southworth and L Young, *Phys. Rev.* **A54**, 2127 (1996)
[5] O Hemmers, G Fisher, P Glans, D L Hansen, H Wang, S B Whitfield, D W Lindle, R Wehlitz, J C Levin, I A Sellin, R C C Perera, E W B Dias, H S Chakraborty, P C Deshmukh and S T Manson, *J. Phys.* **B30**, L727 (1997)

[6] J Jimenez-Mier, S J Schaphorst, C D Caldwell and M O Krause, *Phys. Rev.* **A56**, 3659 (1997)
K Schulz, M Domke, R Pültner, A Gutiérrez, G Kaindl, G Miecznik and C H Green, *Phys. Rev.* **A54**, 3095 (1996)
D W Lindle, P A Heinmann, T A Ferret, M N Paincastelli and D A Shirley, *Phys. Rev.* **A35**, 4605 (1987)
[7] E T Kennedy and I Gray (private communication)
[8] W R Johnson and C D Lin, *Phys. Rev.* **A20**, 964 (1979)
W R Johnson, C D Lin, K T Cheng and C M Lee, *Phys. Scr.* **21**, 409 (1980)
[9] P C Deshmukh, V Radojević and S T Manson, *Phys. Rev.* **A45**, 6339 (1992)
P C Deshmukh and S T Manson, *Phys. Rev.* **A28**, 209 (1983)
[10] N Shanthi and P C Deshmukh, *J. Phys.* **B23**, 61 (1990)
N Shanthi, P C Deshmukh and S T Manson, *Phys. Rev.* **A37**, 4720 (1988)
[11] K-N Huang, *Phys. Rev.* **A22**, 223 (1980)
[12] Most general photon polarization can be described by the density matrix:

$$\rho = \frac{1}{2}\begin{bmatrix} 1 + p\sin 2\alpha & -p\exp(-i2\gamma)\cos 2\alpha \\ -p\exp(i2\gamma)\cos 2\alpha & 1 - p\sin 2\alpha \end{bmatrix},$$

where $\alpha = 0$ represents linear polarization, $\alpha = \pm\pi/4$ represent right and left circular polarizations and any other value of α within its range denotes elliptic polarization. γ specifies the azimuthal orientation of the polarization
[13] E W B Dias, PhD thesis, *Theoretical analysis of photoabsorption processes in some closed shell atoms and ions* (Indian Institute of Technology, Chennai, 1998)
[14] E W B Dias, H S Chakraborty, P C Deshmukh, S T Manson, O Hemmers, G Fisher, P Glans, D L Hansen, H Wang, S B Whitfield, D W Lindle, R Wehlitz, J C Levin, I A Sellin and R C C Perera, *Phys. Rev. Lett.* **78**, 4553 (1997)
[15] H S Chakraborty, P C Deshmukh and S T Manson, to be presented in the *12th International Conference on Vacuum Ultraviolet Radiation Physics*, August 3–7, 1998, California, USA
[16] C M Lee and W R Johnson, *Phys. Rev.* **A22**, 979 (1980)
[17] E W B Dias, H S Chakraborty, P C Deshmukh and S T Manson, *Phys. Rev.* (submitted)
[18] P C Deshmukh, H S Chakraborty, E W B Dias and S T Manson, to be published